SHALLOW WATER SEAGRASS OBSERVED BY HIGH RESOLUTION FULL WAVEFORM BATHYMETRIC LIDAR

Zhigang Pan, Juan Carlos Fernandez-Diaz, Craig L. Glennie, Michael Starek

Civil and Environmental Engineering, University of Houston
National Center for Airborne Laser Mapping
Harte Research Institute for Gulf of Mexico Studies, Texas A&M University at Corpus Christi

ABSTRACT

Full waveform bathymetric LiDAR allows a detailed examination of laser backscatter from the water surface, water column and benthic layer. The presence of seagrass on the benthic layer would also be expected to influence the backscattered radiation encapsulated in the full waveform observations. The combination of conventional geometric features, radiometric features and derived geometric features from the waveform analysis may make it possible to identify the presence of seagrass or even classify the different types of seagrass. An analysis of the correlation of seagrass location with different full waveform LiDAR parameters is presented. Overall, it is found that a high degree of correlation exists between the presence of seagrass and LiDAR intensity, benthic elevation and benthic return pulse width. Surface roughness, curvature and vertical uncertainty are found to have weak correlation with the presence of seagrass.

Index Terms— LiDAR, Bathymetry, Seagrass, Full waveform

1. INTRODUCTION

Discrete Light Detection and Ranging(LiDAR) has become a popular surveying technique to obtain 3D target or topographic information in recent years[1]. Airborne LiDAR bathymetry(ALB) is increasingly used in nautical charting, navigation and coastal surveying. ALB systems contain a laser that emits a blue-green laser beam, which can penetrate through the water surface and get LiDAR returns from the subsurface and submerged objects[2]. Seagrass is submerged vegetation that plays a key role in aquatic ecosystems by providing habitats, trapping sediments and slowing water flow for other biological species. It also provides the food and living environments for diverse species and can be used to investigate fisheries health and waste treatment[3]. Monitoring seagrass regularly is therefore an important environmental initiative; however obtaining 3D metrics of seagrass over large areas via traditional in-situ techniques is time consuming and expensive.

Emergent bathymetric LiDAR sensors and waveform processing algorithms make it possible to extract 3D measurements in these previously inaccessible shallow water environments. Full waveform LiDAR assists in this regard as it records the full backscattered echoes which enables the possibility to extract more information about the target and propagation medium[4]. However, seagrass still presents a challenge, as is most seagrass has a height of less than 0.5m, which is beneath the vertical resolution in the return pulse, and hence echoes from the seagrass and benthic laser overlap as a single peak return waveform[5]. Despite these challenges, the presence of seagrass can still disturb or stretch the return waveform shape. In this paper, we present the radiometric and geometric features derived from full waveform bathymetric LiDAR and the derived point cloud to investigate their potential for seagrass identification and mapping. By combining the features with passive optical sensors, such as hyperspectral imagers, the preliminary results show great potential for characterizing the presence of seagrass from remotely sensed bathymetric LiDAR data.

2. LIDAR WAVEFORM ANALYSIS

Full waveform LiDAR has been widely analyzed in both topographic and bathymetric applications. For example, for topography, full waveform was used to determine forest inventory and biomass, especially for the detection of low vegetation that discrete LiDAR returns was unable to identify[6]. In bathymetry, the fusion of the passive hyperspectral imagery and active full waveform LiDAR has helped to improve both the detection and classification of object under water surfaces, water column scattering properties and water depth measurements[7, 8]. However, shallow water LiDAR bathymetry full waveform processing has a number of challenging characteristics; for instance the signal returns from the water surface, water column and the benthic layers returns overlap both temporally and spatially. There have been previous attempts to solve the mixture by applying the NIR(topographic) waveform processing techniques to the shallow water waveforms[9]. However the widely used

method for topographic waveform processing, Gaussian decomposition, performs poorly when trying to separate the highly overlapped returns from water surface, water column and benthic layer[10]. For Gaussian decomposition, a good initial guess of the number of components and approximate temporal locations of the return pulse peaks and widths are required[11]. Because shallow water bathymetry is very complex it is not easy to satisfy these requirements. As a viable alternative, for this work we have employed a continuous wavelet transform (CWT) to process the full waveform LiDAR return signal. The CWT has the advantage that it does not require an initial guess of peak locations and widths; it is an iterative method to check for all possible peak locations based on transformation parameters.

3. DATASET, DATA PROCESSING AND ANALYSIS

Our study area is located within Redfish Bay near Corpus Christi, TX, and it is composed of mostly very shallow water (<2m)(Fig 1.). The area is a scientific preserve where seagrass can grow relatively uninhibited by human activities. Seagrass present in Redfish Bay consists primarily of three different seagrass species: thalassia, halodule, and syringodium, macroalgae is also present. Most of the seagrass

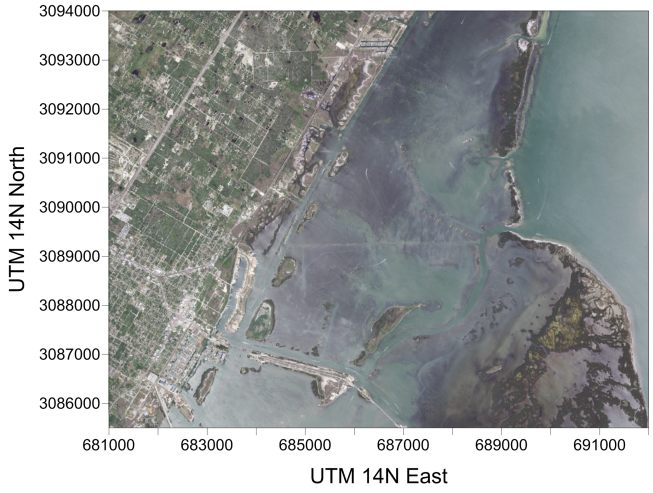

Fig. 1. Overview of Red Fish Bay in Corpus Christi

is less than 0.5m in vertical height and while this may not result in individual LiDAR echoes, it is expected that some of the waveform features could detect the presence of seagrass. Data for this study was collected by the National Center for Airborne Laser Mapping (NCALM) using an Optech Aquarius system in Sept, 2012. Full waveform was recorded with a 1 GHz digitizing frequency at 12 bits resolution. Only a single flightline was recorded with full waveform information, and therefore no overlap area at the swath edges were recorded. The laser was flown with a slight forward tilt to attempt to mitigate specular reflections at nadir from the water surface. Primary flight and sensor information is given in Table 1.

A Continuous Wavelet Transformation (CWT) was used

Table 1. Airborne Acquisition Parameters

Operating altitude	500m(nominal)
Aircraft speed	60m/s(nominal)
Scanning rate	35kHz
Beam divergence	1mrad
Forward tilt angle	5°
Scan angle	$\pm 24.2^\circ$
Swath width	450m
Point density	$1.298 pts/m^2$

to find return peaks and the peaks location were then fed into Expectation-Maximization (EM) algorithm to estimate the pulse width. In Table 2 the waveform shots represents

Table 2. Waveform processing result specification

	Waveform (pts)	Discrete (pts)
Waveform shots	3,808,187	
Total points	4,355,334	
Lost points	49,060	
Actual points	4,306,274	3,803,958
Only 1 return	3,206,068	3,777,103
2 returns	549,918	13,396
3 returns	122	21
$\geq$4 returns	1	0

the total number of waveform processed, and total points is the total potential points detected by waveform processing. Lost points are points discarded because of missing georeferencing information and actual points are the points detected and georeferenced. From the actual points, about 13.21% more points were detected in the waveform. From the return numbers, over 14.44% of returns in waveform records have been broken into separate returns comparing at 0.35% for discrete records, which shows that a significant amount of the full waveform processing has been able to resolve multiple returns not detected by the discrete processing.

In order to inspect the ability of full waveform to detect the presence of seagrass, different features have been derived from the waveform/point cloud:

• Ground elevation (Ele): is the elevation of ground returns after removal of the water surface;

• Ground intensity (Int): is derived from the full waveform by removing the return gate and derived from the EM estimated pulse amplitude;

• Ground pulse width (Pul): is the standard derivation of the pulse width estimated by EM, normalized with respect to return intensity;

• Roughness (Rou): is a local parameter defined as the distance from a point to the plane formed by its neighbors within

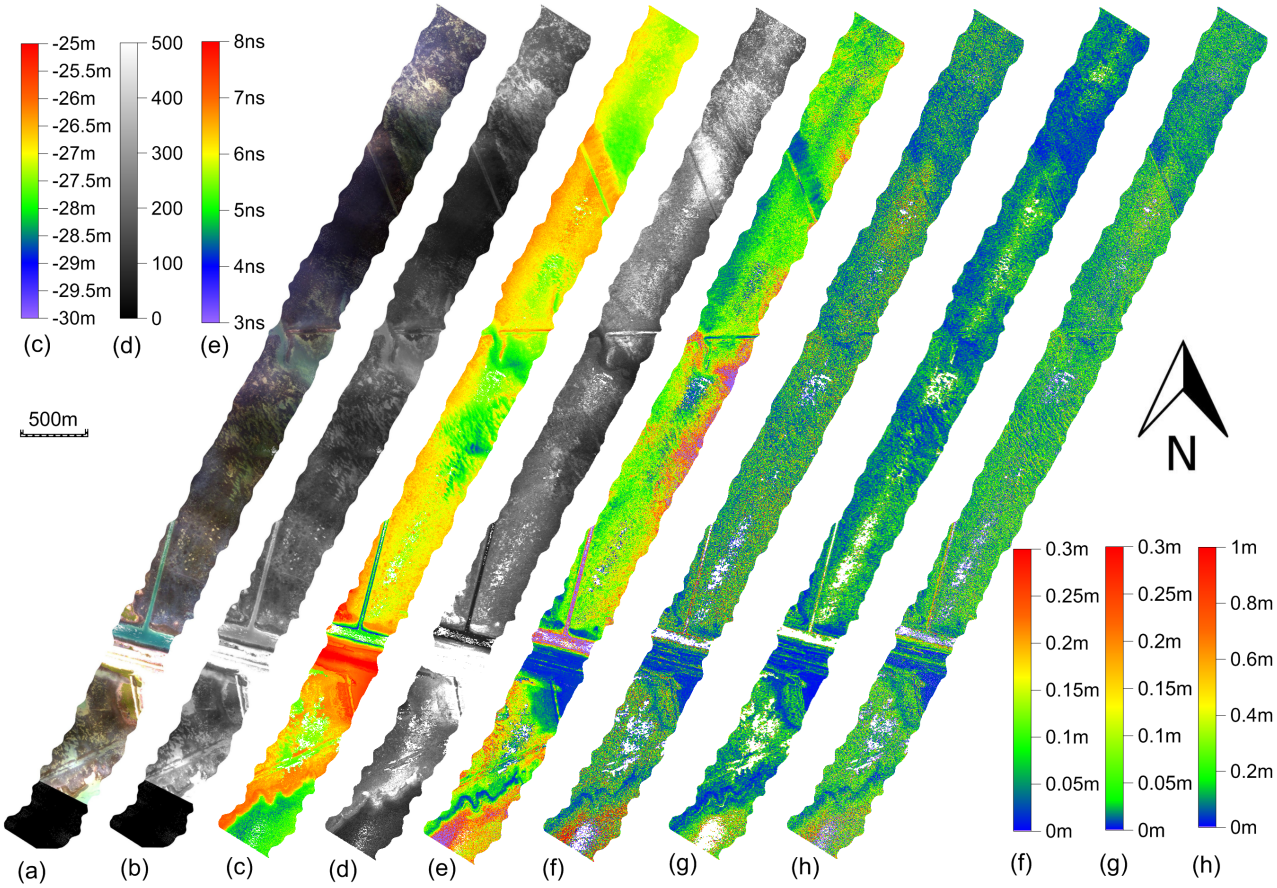

Fig. 2. Features presenting seagrass with RGB imagery from passive optical camera (a),532nm intensity imagery from passive optical camera (b), ground points (filtered) elevation map (ellipsoidal height referring to WGS84) (c), ground points intensity map (d), ground returns pulse width (e), roughness for local planes (f), curvature for local planes (g), local vertical height(f).

a 3m radius;

• Mean curvature (Cur): is a local parameter defined as the mean curvature with radius of 3m;

• Vertical uncertainty (Ver): is vertical elevation difference comparing to the lowest point within a 3m grid.

Results for all of these paramters are displayed in Figure 2. An examination of Fig 2 shows that elevation and intensity maps show some clusters which might be seagrass; pulse width map shows possible disturbances along the laser path; longer pulse widths could be caused by both the water depth (turbidity) or seagrass presence causing multiple backscattering echoes. Roughness and curvature maps depict the local geometric features as larger roughness and curvature would be expected for seagrass presence. Finally, vertical uncertainty could possibly show similar feature as roughness with larger uncertainty for seagrass locations.

A simple Pearsons correlation analysis was conducted including the passive hyperspectral imagery band at a wavelength of 532nm (Pas) to examine the underlying correlation of each feature derived from full waveform LiDAR,; the results are displayed in Table 3. The correlations of the local region features to passive imagery (roughness, curvature, and vertical uncertainty) are lower than the those for pulse width, elevation and intensity, suggesting that a combination of these waveform derived features would be good parameters for detection of seagrass presence.

Table 3. Pearson's correlation for each feature

	Ele	Int	Pul	Rou	Cur	Ver	Pas
Ele	1.00	0.28	0.10	0.08	0.13	0.27	0.25
Int	0.28	1.00	0.51	0.23	0.09	0.19	0.45
Pul	0.10	0.51	1.00	0.06	0.01	0.11	0.21
Rou	0.08	0.23	0.06	1.00	0.42	0.24	0.07
Cur	0.13	0.09	0.01	0.42	1.00	0.24	0.03
Ver	0.27	0.19	0.11	0.24	0.24	1.00	0.09
Pas	0.25	0.45	0.21	0.07	0.03	0.09	1.00

ENVI 4.8 was used to classify all the six features from the full waveform bathymetric LiDAR data with supervised Min-

imum Distance (MD) method. Unfortunately, only 9 points of ground truth were collected within the full waveform flightline extent. In the vicinity of the ground truth data, 9081 pixels were chosen for supervised training data, which is about 0.28% of the entire data area. Three classes were chosen, ground (including features above water surface), sand (benthic ground) and grass; the statistics of classification was shown in table 4. From the Table, the grass under water surface is still disturbing the classification of the bare benthic returns and the ground returns, but the overall accuracy can be up to 75%, and is encouraging despite the lack of in situ ground control for this comparison.

Table 4. Statistics of the supervised classification

Over all accuracy	74.5987%			
	Ground Truth(Percent)			
Class	Grass	Sand	Ground	Total
Unclassified	0.00	0.00	0.00	0.00
Grass	75.81	28.77	22.43	29.60
Sand	16.58	71.23	0.00	29.03
Ground	7.61	0.00	77.57	41.37
Total	100.00	100.00	100.00	100.00

4. CONCLUSION

This study has assessed the ability of full waveform bathymetric LiDAR in shallow water to detect the presence of seagrass. With proper waveform processing algorithms, better separation of water surface return and benthic returns can be achieved, which shows promise to improve the identification of seagrass under shallow water. Different features have been derived from the full waveform data. At first analysis, the pulse width, elevation and return intensity show good correlation with the presence of seagrass. A simple supervised classification shows approximately 75% accuracy however the benthic features (grass and sand) disturb the results making it more difficult to discriminate each class. However, the preliminary results still show that full waveform has the capability to describe the features for very shallow water and assist in discriminating different classes. Further work with more ground truth data is needed to validate the results and combine the active features to the passive observations for enhanced automated seagrass identification.

5. REFERENCES

[1] C. L. Glennie, W. E. Carter, R. L. Shrestha, and W. E. Dietrich, "Geodetic imaging with airborne LiDAR: the Earth's surface revealed," *Reports on Progress in Physics*, vol. 76, no. 8, p. 86801,

[2] J. C. Fernandez-Diaz, C. L. Glennie, W. E. Carter, R. L. Shrestha, M. P. Sartori, A. Singhania, C. J. Legleiter, and B. T. Overstreet, "Early Results of Simultaneous Terrain and Shallow Water Bathymetry Mapping Using a Single-Wavelength Airborne LiDAR Sensor," *IEEE Journal of Selected Topics in Applied Earth Observations and Remote Sensing*, vol. 7, no. 2, pp. 623–635,

[3] C. M. Duarte, "Seagrass ecology at the turn of the millennium: challenges for the new century," *Aquatic Botany*, vol. 65, no. 1-4, pp. 7–20,

[4] C. Mallet and F. Bretar, "Full-waveform topographic lidar: State-of-the-art," *ISPRS Journal of Photogrammetry and Remote Sensing*, vol. 64, no. 1, pp. 1–16,

[5] C. E. Parrish, J. N. Rogers, and B. R. Calder, "Assessment of Waveform Features for Lidar Uncertainty Modeling in a Coastal Salt Marsh Environment," *IEEE Geoscience and Remote Sensing Letters*, vol. 11, no. 2, pp. 569–573,

[6] F. Pirotti, "Analysis of full-waveform LiDAR data for forestry applications: a review of investigations and methods," *iForest - Biogeosciences and Forestry*, vol. 4, no. 3, pp. 100–106,

[7] G. Tuell, K. Barbor, and J. Wozencraft, "Overview of the coastal zone mapping and imaging lidar (CZMIL): a new multisensor airborne mapping system for the U.S. Army Corps of Engineers," *Proceedings of SPIE - The International Society for Optical Engineering*, vol. 7695, pp. 76 950R–76 950R–8,

[8] J. Y. Park, V. Ramnath, V. Feygels, M. Kim, A. Mathur, J. Aitken, and G. Tuell, "Active-passive data fusion algorithms for seafloor imaging and classification from CZMIL data," in *SPIE Defense, Security, and Sensing*. International Society for Optics and Photonics, 2010, p. 769515.

[9] T. Allouis, J.-S. Bailly, Y. Pastol, and C. Le Roux, "Comparison of LiDAR waveform processing methods for very shallow water bathymetry using Raman, near-infrared and green signals," *Earth Surface Processes and Landforms*, vol. 650, no. January, pp. n/a–n/a,

[10] C. E. Parrish, I. Jeong, R. D. Nowak, and R. Brent Smith, "Empirical comparison of full-waveform lidar algorithms: Range extraction and discrimination performance," *Photogrammetric Engineering and Remote Sensing*, vol. 77, no. 8, pp. 825–838,

[11] W. Wagner, A. Ullrich, V. Ducic, T. Melzer, and N. Studnicka, "Gaussian decomposition and calibration of a novel small-footprint full-waveform digitising airborne laser scanner," *ISPRS Journal of Photogrammetry and Remote Sensing*, vol. 60, no. 2, pp. 100–112,